Punctiform and Polychromatic Pre-Descemet Corneal Dystrophy: Clinical Evaluation and Identification of the Genetic Basis

JORGE L. ALIÓ DEL BARRIO, DOUG D. CHUNG, OLENA AL-SHYMALI, ALICE BARRINGTON, KAVYA JATAVALLABHULA, VINAY S. SWAMY, PILAR YÉBANA, MARIA ANGÉLICA HENRÍQUEZ-RECINE, ANA BOTO-DE-LOS-BUEIS, JORGE L. ALIÓ, AND ANTHONY J. ALDAVE

• PURPOSE: **This study reports the clinical features and genetic bases of 3 previously unreported families with punctiform and polychromatic pre-Descemet corneal dystrophy (PPPCD).**

• DESIGN: **Observational case series.**

• METHODS: **Full ophthalmic assessment was performed for members of 3 unreported families with PPPCD. Structural and biomechanical alterations of the cornea were screened. Whole exome sequencing (WES) was performed in the first family. Novel or rare variants that segregated with the affected status were screened in the other 2 families using Sanger sequencing. Identified variants that segregated with the affected status in all families were characterized by using in silico prediction tools and/or in vitro splice assays. Additionally, 2 previously reported PPPCD families were screened for variants identified in the 3 unreported PPPCD families.**

• RESULTS: **PPPCD was diagnosed in 12 of the 21 examined members of the 3 unreported families. The only refractive, topographic, or biomechanical abnormality associated with PPPCD was a significantly increased corneal stiffness. WES and Sanger sequencing identified 2 variants that segregated with the affected status in all 3 families: a rare intronic *PDZD8* c.872+10A>T variant and a novel missense *PRDX3* c.568G>C (p.Asp190His) variant. The same *PRDX3* variant was identified in the previously reported PPPCD family expressing the common PPPCD phenotype and was predicted by in silico prediction tools to be damaging to protein function.**

• CONCLUSIONS: **PPPCD is associated with an alteration of corneal biomechanics and a novel missense variant in *PRDX3*. Screening of additional families will determine whether all families demonstrate a *PRDX3* variant or whether locus heterogeneity may exist for PPPCD. (Am J Ophthalmol 2020;212:88–97. © 2019 Elsevier Inc. All rights reserved.)**

PUNCTIFORM AND POLYCHROMATIC PRE-DESCEMET corneal dystrophy (PPPCD) is a rare corneal dystrophy first described by Fernandez-Sasso and associates in 1979.[1] Typically asymptomatic and without any reported visual disturbance, PPPCD is characterized by the presence of punctiform, multicolored opacities in the posterior stroma, immediately anterior to Descemet's membrane.[1–7] According to the second edition of the International Classification of Corneal Dystrophies (IC3D), PPPCD is currently considered a subtype of pre-Descemet corneal dystrophy (PDCD), which is classified as a category 4 dystrophy (suspected, new, or previously documented corneal dystrophies, where the evidence as a distinct entity was not yet convincing).[8]

To the best of the present authors' knowledge, only 10 families with PPPCD have been reported in the medical literature as case reports (Table 1).[1–7] Although an autosomal dominant inheritance has been suggested, the inheritance pattern and genetic basis have yet to be elucidated. Additionally, it is also unknown whether PPPCD is associated with any other corneal abnormalities as a complete ophthalmic assessment of individuals with PPPCD has not been reported.

This study presents 3 previously unreported PPPCD pedigrees in which a comprehensive ophthalmic assessment of affected and unaffected family members was performed and the results of whole-exome sequencing (WES) and Sanger sequencing in these and 2 previously reported pedigrees to identify the genetic basis of PPPCD.

SUBJECTS AND METHODS

THREE PREVIOUSLY UNREPORTED PPPCD PEDIGREES (PPPCD in family 1, family 2, and family 3) and 2 previously reported pedigrees (PPPCD family 4 and family 5)[7] were

AJO.com Supplemental Material available at AJO.com.
Accepted for publication Nov 19, 2019.

From the Cornea, Cataract and Refractive Surgery Unit (J.L.AdB., O.A-S., P.Y., J.L.A) Vissum Corporación, Alicante, Spain; Division of Ophthalmology (J.L.AdB., J.L.A.), School of Medicine, Universidad Miguel Hernández, Alicante, Spain; Stein Eye Institute (D.D.C., A.B., K.J., V.S.S., A.J.A.), David Geffen School of Medicine, University of California Los Angeles, Los Angeles, California, USA; and the Ophthalmology Department (M.A.H-R., A.B-d-l-B.), La Paz University Hospital, Madrid, Spain.

Inquiries to: Dr. Anthony J. Aldave, Stein Eye Institute, University of California Los Angeles, 200 Stein Plaza, Los Angeles, California 90095-7003, USA; e-mail: aldave@jsei.ucla.edu

0002-9394/$36.00
https://doi.org/10.1016/j.ajo.2019.11.024

TABLE 1. Description of Families Reported to Have Punctiform and Polychromatic Pre-Descemet Corneal Dystrophy in Published Studies

Family	Study	Country	Publication Year	Affected Members	Proposed Inheritance	Family Origin
1	Fernández-Sasso et al[1]	Argentina	1979	8	Autosomal dominant	French/Spanish Pyrenees
2	Lisch et al[6]	Germany	1984	2	Autosomal dominant	Not reported
3	Tzelikis et al[5]	Brazil	2007	3	Autosomal dominant	Not reported
4		Brazil	2007	1 (family members not analyzed)	Not reported	Not reported
5	Dolz-Marco et al[3]	Spain	2013	2	Autosomal dominant	Eastern Spain
6	Coelho et al[4]	Brazil	2015	1 (family members not analyzed)	Not reported	Not reported
7		Brazil	2015	1 (family members not analyzed)	Not reported	Not reported
8	Lagrou et al[2]	Canada	2016	3	Autosomal dominant	Columbia (ancestral family from Northern Spain)
9	Henríquez Recine et al[7]	Spain	2018	8	Autosomal dominant	Central Spain
10		Spain	2018	3	Autosomal dominant	Central Spain
11	Alió del Barrio et al (present study)	Spain	2019	9	Autosomal dominant	Eastern Spain
12		Spain	2019	3	Autosomal dominant	Eastern Spain
13		Spain	2019	1	Insufficient Sample	Eastern Spain

identified, and family members were enrolled in this observational case series and in the authors' ongoing study of inherited ocular disorders. Informed written consent was obtained from all subjects in this study according to the tenets of the Declaration of Helsinki, and approval for this study was obtained from the Institutional Review Board at the University of California at Los Angeles (UCLA IRB 11–000020) and the ethical committee from Vissum Corporación.

• **CLINICAL EVALUATION:** All affected and unaffected individuals from 3 previously unreported families (PPPCD families 1-3) who agreed to participate in the study received full ophthalmic examinations including slit lamp biomicroscopy, fundoscopy, corneal endothelial specular microscopy (Noncon Robo, Konan, Hyogo, Japan), corneal topography (including anterior keratometry, pachymetry and corneal aberrometry with 6-mm pupil) (Sirius, CSO, Firenze, Italy), ocular aberrometry (Osiris, CSO), anterior segment optical coherence tomography (OCT) (model MS-39, CSO), corneal biomechanics (ocular response analyzer, OftalTech, Barcelona, Spain) and ocular scattering index (high definition analyzer, Visiometrics, Barcelona, Spain). Affected individuals also underwent corneal confocal biomicroscopy (Confoscan 4, Nidek, Aichi, Japan). Two individuals under 5 years of age were included in the study, but due to the expected lack of cooperation, only a clinical examination (slit lamp examination and fundoscopy) was performed. The diagnosis of PPPCD was based on the presence of polychromatic crystals located in the posterior corneal stroma (in a pre-Descemet membrane location) on slit lamp examination that appeared as hyperreflective pre-Descemet opacities with confocal and specular microscopy (Figures 1 and 2).

Although a comprehensive medical history, including medications, was taken from each of the individuals recruited in the study, a physical examination to identify systemic or metabolic associations was not performed, given the last of evidence of extraocular manifestations of PPPCD in previous reports.[1–7]

• **STATISTICAL ANALYSIS:** SPSS version 22.0 software (IBM SPSS, Armonk, New York) for Windows (Microsoft, Redmond, Washington) was used for statistical analysis. Analysis was performed for all variables using nonparametric tests due to the small sample size ($n < 30$). Thus, the Mann-Whitney *U* test was applied to assess differences between groups (affected and unaffected), except for the nominal variable "sex," category, for which the Pearson chi-squared test was used. Differences were considered statistically significant when P was <0.05.

• **DNA ISOLATION:** After informed consent was obtained, saliva samples were collected from member of each of the 3 unreported families and the 2 previously reported families,[7] using a saliva collection kit (Oragene DNA kit; Genotek, Inc., Ottawa, Ontario, Canada), and genomic DNA was isolated using the Oragene prepIT-L2P kit (Genotek, Inc.) according to the manufacturer's instructions.

• **WES AND VARIANT CALLING:** WES was performed using genomic DNA derived from affected and unaffected members of PPPCD family 1. DNA libraries were prepared using the TruSeq DNA sample preparation kit version 2

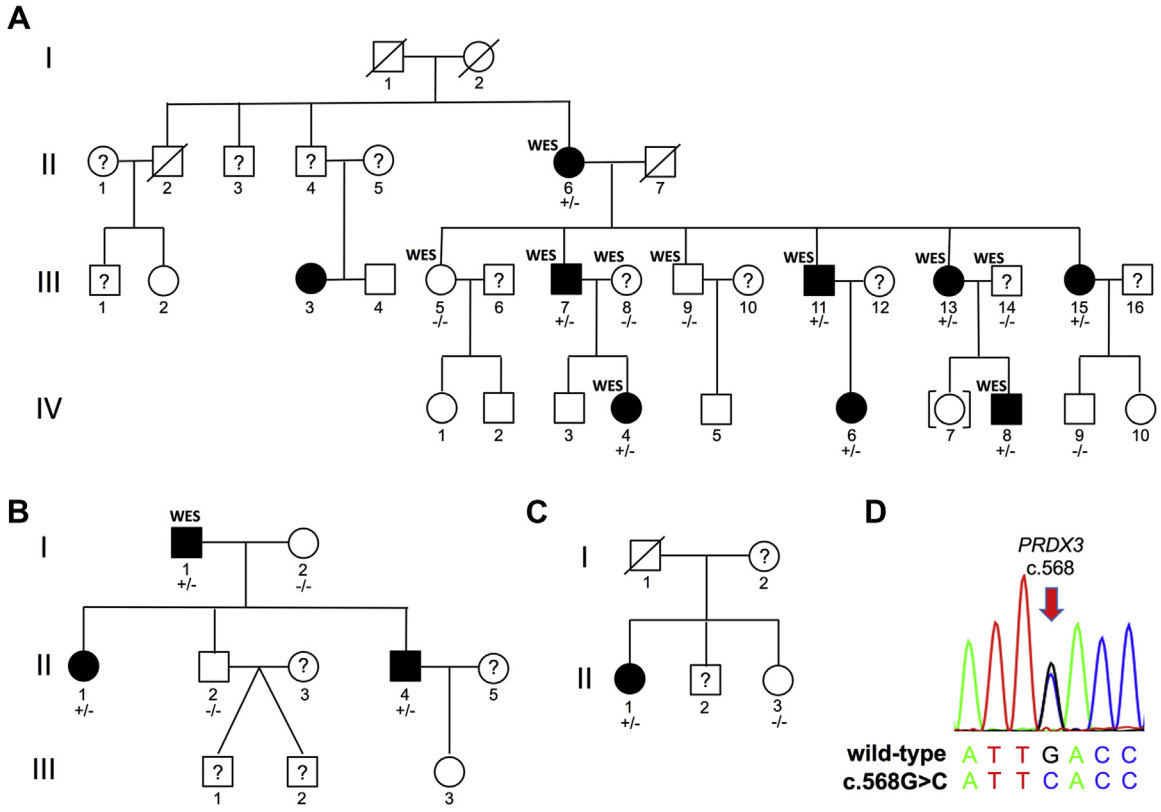

FIGURE 1. Pedigrees of 3 previously unreported Spanish PPPCD families. (A) Family 1, family 2 (B), and family 3 (C) with punctiform and polychromatic pre-Descemet corneal dystrophy. Question marks (?) indicate unexamined individuals. Whole-exome sequencing (WES) indicates individuals in whom whole exome sequencing was performed. Individuals heterozygous for the *PRDX3* c.568G > C variant are indicated by +/−, and individuals who lack the variant are indicated by −/−. (D) The heterozygous *PRDX3* c.568G > C variant (Refseq accession NM_006793.4) was confirmed by Sanger sequencing in all affected individuals.

(Illumina Inc., San Diego, California), and exome capture was performed using the SeqCap EZ Exome Library version 3.0 (Roche NimbleGen, Inc., Madison, Wisconsin). Paired-end sequencing (2 × 150 base pairs [bp]) was performed using HiSeq 4000 (Illumina). The Biomedical Genomics Workbench 5.0 (Qiagen, Redwood City, California) was used to generate sequence reading aligned to the Hg38 human genome reference, and aligned readings were annotated with the Ensembl 88 transcript database (Oaxaca, Mexico). Called variants were annotated using the Single Nucleotide Polymorphism Database 150 database (US National Institutes of Health/National Center for Biotechnology Information, Bethesda, Maryland).

• **FILTERING OF WES VARIANTS:** Ingenuity Variant analysis software (Qiagen) was used to analyze variants found by WES analysis in family 1, and affected members and unaffected members of PPPCD family 1 were filtered to exclude any variant with: a quality score <20, a read count <5, or a minor allele frequency (MAF) >0.5% in either the Exome Aggregation Consortium (ExAC), 1,000 genomes, or gnomAD databases; present in a homozygous state; absent in any of the affected individuals; and present in any of the unaffected individuals. To make allowances for a potential false positive or false negative call by WES for any particular variant in 1 individual, additional filtering and analyses were performed to exclude variants: absent in 2 or more of 6 affected and present in any unaffected individuals; or absent in any of the affected individuals and present in 2 or more of 4 unaffected individuals.

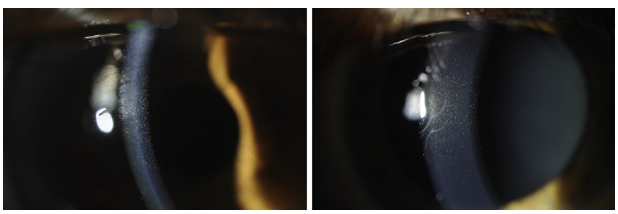

FIGURE 2. Slit lamp photomicrographs of an individual with punctiform and polychromatic pre-Descemet corneal dystrophy. Slit lamp photomicrographs of an individual with punctiform and polychromatic pre-Descemet corneal dystrophy (Figure 1A: individual III-15) demonstrating multiple polychromatic posterior stromal opacities in each eye.

• **PCR AMPLIFICATION AND SANGER SEQUENCING:** Primers were designed to amplify the genomic regions containing filtered variants identified by WES; exons and/or introns of *PDZD8* (NCBI Reference Sequence Database [Refseq Gene ID]: 118987; NIH, Bethesda, Marylan), *PRDX3* (Refseq Gene ID: 10935), and *OR2M5* (Refseq gene ID: 80000) (Supplemental Table 1 for primer sequences); and variants used for mini-haplotype analysis. DNA amplification by polymerase chain reaction (PCR) was performed in 25-μL reaction volumes containing 25-40 ng of genomic DNA, 2.5 pmol of each primer, and GoTaq Green Master mixture (Promega, Madison, Wisconsin) according to the manufacturer's recommendations. The PCR protocol consisted of a denaturizing step at 95°C for 3 minutes, followed by 35× cycle of a denaturing step at 95°C for 30 seconds, an annealing step at 60°C for 30 seconds, and an elongation step at 72°C for 30-60 seconds. Sanger sequencing was performed by Laragen, Inc. (Culver City, California).

• **IN SILICO VARIANT PREDICTION AND SCORING:** Filtered variants identified by WES were analyzed by online tools SIFT (San Francisco, California),[9] Polyphen-2 (Harvard, Cambridge, Massachusetts),[10] CADD (Baltimore, Maryland),[11,12] Provean,[13] and/or Human Splicing Finder (Marseilles, France)[14] to predict each variant's impact on protein function or splicing.

• **MINI-HAPLOTYPE ANALYSES:** To determine the haplotype of the genomic region encompassing the *PRDX3* c.568G>C variant on chromosome 10, rare proximal variants were identified in the WES data from PPPCD family 1 and screened in affected individuals from families 2-4 who harbored the *PRDX3* c.568G>C variant (Supplemental Table 1 for primer sequences).

• **IN VITRO SPLICE ASSAY:** A 1444-bp region of *PDZD8* containing either the wild-type sequence or the c.872+10A>T variant was amplified from genomic DNA obtained from either an affected or unaffected individual of PPPCD family 1. The amplified *PDZD8* fragment contained exon 1, along with 264 bp of the 5′ untranslated region (UTR) and 308 bp of intron 1 that flank exon 1, and was amplified using the following primer sequences: forward- 5′-GAATTCCCATATGGAGTGGAGGCCTG AGGGA-3′ and reverse- 5′-GAATTCCCATATGCCT GGGGATTAGGGTAGGCT-3′. Both primers were designed with a NdeI restriction site at their 5′ ends to be used for cloning the amplified *PDZD8* fragment into the pTBNde (min) plasmid (plasmid 15125, a gift from Franco Pagani, Addgene, Cambridge, Massachusetts) that contains a modified version of the α-globin-fibronectin-EDB minigene.[15,16]

The splicing assay was performed by transfecting HEK293T cells with each minigene plasmid using Lipofectamine LTX (Life Technologies, Grand Island, New York) according to the manufacturer's recommended protocols. Total RNA from transfected HEK293T was extracted using TRI reagent (Sigma-Aldrich Corp., St. Louis, Missouri), and complementary DNA (cDNA) was synthesized using the SuperScript III First-Strand kit (Life Technologies) according to the manufacturer's recommendations. Reverse transcription PCR (RT-PCR) was performed using previously published RT-PCR protocols with primers targeting the flanking fibronectin exons (Supplemental Table 1 shows primer sequences).[17]

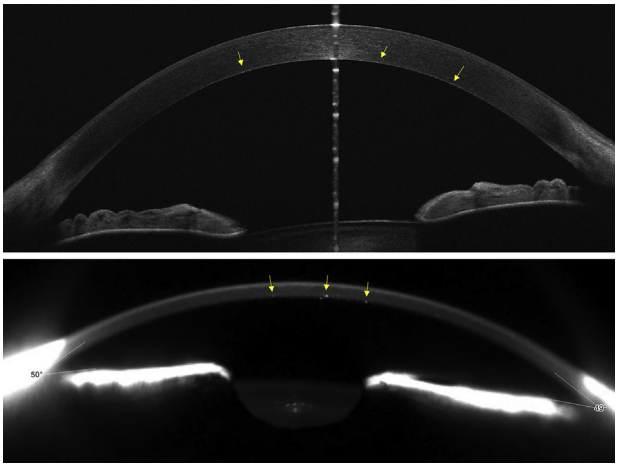

FIGURE 3. Anterior segment OCT and Scheimpflug imaging. Anterior segment OCT (top) and Scheimpflug (bottom) imaging of an individual with punctiform and polychromatic pre-Descemet corneal dystrophy (Figure 1A: individual III-11) demonstrating hyperreflective posterior stromal opacities (yellow arrows) that are more easily identified with Scheimpflug imaging. OCT = optical coherence tomography.

RESULTS

• **CLINICAL EVALUATION OF PPPCD FAMILIES:** Seventeen members from family 1, six members from family 2, and two members from family 3 were enrolled in the clinical study (Figure 1). Slit lamp examination demonstrated bilateral, symmetric, punctiform and polychromatic opacities in the deep stroma immediately anterior to Descemet membrane in eight individuals from family 1, three individuals from family 2, and one individual from family 3 (Figures 1 and 2). There were no significant differences in mean ages between the affected (42.9 years of age; range, 8-79 years) and unaffected (33.3 years of age; range, 1-69 years) individuals ($P = 0.25$) or in the percentage of men in the affected (41.6% [5 of 12]) and unaffected (53.8% [7 of 13]; $P = 0.38$) groups.

Comprehensive clinical examination failed to reveal associated ophthalmic disorders in the affected individuals. In addition, no ophthalmic surgical interventions were documented in any of the study patients' medical records,

TABLE 2. Clinical Evaluation of PPPCD Families

	PPPCD Affected		Unaffected		
	Mean	SD	Mean	SD	*P* Value
Refractive					
Ref Sphere, D	−0.42	2.54	−2.08	3.26	0.12
Ref cylinder, D	−0.79	0.66	−0.48	0.45	0.1
CDVA, decimal	0.1	0.05	1.02	0.06	0.43
Tomographic					
Anterior Km, D	44.33	1.93	43.94	1.35	0.67
Topo cylinder, D	−0.98	0.5	−1.13	0.44	0.2
CCT, μm	528.65	30.69	539.4	25.48	0.24
Thinnest, μm	517.75	32.81	530.15	28.27	0.21
Kmax, D	44.83	1.96	44.51	1.43	0.74
Wavefront					
Corneal total HOA, μm	0.59	0.37	0.46	0.1	0.35
Corneal coma, μm	0.33	0.18	0.31	0.1	0.95
Corneal sph, μm	0.22	0.18	0.22	0.07	0.11
Endothelial specular microscopy					
CD, cells/mm^2	2,563	708.7	2,572	344.83	0.84
CV	43	40.3	33	5.56	0.12
Hexagonality, %	61	10.13	61	9.26	0.48
Ocular abberometry					
Strehl ratio, PSF	0.37	0.15	0.39	0.17	0.85
OSI	1.24	1.19	0.82	0.53	0.62
Biomechanical					
CH, mm Hg	10.32	1.44	9.85	1.52	0.26
CRF, mm Hg	10.77	1.32	9.93	1.24	0.02[a]
Intraocular pressure, mm Hg	14.6	3.5	13.25	2.15	0.22

6A = hexagonality; CCT = central corneal thickness; CD = cell density; CDVA = corrected distance visual acuity; CH = corneal hysteresis; CRF = corneal resistance factor; CV = coefficient of variation; D = diopter; dec = decimal scale; HOA = higher order aberrations; Km = mean keratometry; Kmax = maximum keratometry; OSI = ocular scatter index; PPPCD = punctiform and polychromatic pre-Descemet corneal dystrophy; PSF = point spread function; Ref = refractive; SD = standard deviation; sph = spherical aberration; Thinnest = thinnest pachymetric point; Topo = topographic.

[a]Statistically significant differences.

with the exception of bilateral cataract surgery in an affected 79-year-old individual. Corneal imaging could not be performed due to limited cooperation in 2 patients, a 4-year-old child (unaffected based on slit lamp examination) and a 1-year-old infant (unaffected based on a portable slit lamp examination).

• **ANTERIOR SEGMENT IMAGING:** Anterior segment OCT imaging of the corneas of affected individuals demonstrated faint, hyperreflective, pre-Descemet opacities (Figure 3, top), which were more easily visualized using Scheimpflug imaging (Figure 3, bottom). These opacities were absent in the unaffected individuals.

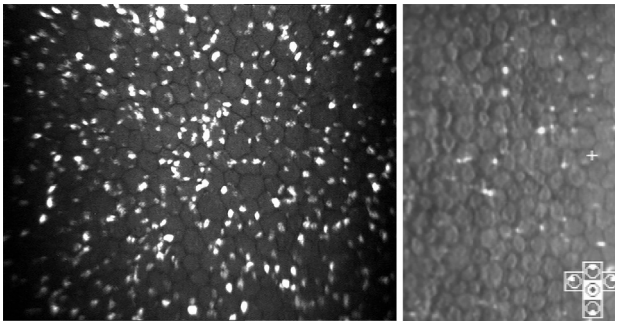

FIGURE 4. Confocal microscopy and specular microscopy imaging. Confocal microscopy (left) and specular microscopy (right) imaging of the posterior corneal stroma of an individual with punctiform and polychromatic pre-Descemet corneal dystrophy (Figure 1B: individual II-4) demonstrate hyperreflective opacities distributed at the level of Descemet membrane.

• **SPECULAR AND CONFOCAL MICROSCOPY IMAGING:** Specular microscopy of the corneal endothelium revealed a normal endothelial cell mosaic in both groups, with similar cellular density, coefficient of variation, and percentage of hexagonality (Table 2). Affected individuals demonstrated multiple, round, hyperreflective opacities at the pre-Descemet level, immediately anterior to an unremarkable endothelial cell layer (Figure 4, right). Confocal microscopy of affected individuals demonstrated an unremarkable corneal stroma other than for the extracellular, pre-Descemet opacities that measured approximately 10 μm in diameter (Figure 4, left).

• **CORNEA BIOMECHANICS:** Corneal biomechanical evaluation demonstrated increased corneal hysteresis ($P = 0.26$) and significantly increased corneal resistance factor ($P = 0.02$) in individuals with PPPCD compared with unaffected individuals (Table 2).

• **VISION, REFRACTION, AND CORNEAL TOPOGRAPHY:** There were no statistically significant differences among any of the other analyzed visual, refractive, keratometric, pachymetric, or corneal aberrometric parameters (Table 2).

• **WES ANALYSIS OF PPPCD FAMILY 1:** DNA samples were collected from 13 members (8 affected and 5 unaffected) of PPPCD family 1 (Figure 1A). WES was performed on DNA samples from six affected (Figure 1A: individuals II:6, III:7, III:11, III:13, IV:4, IV:8) and four unaffected individuals (Figure 1A: individuals III:5, III:8, III:9, III:14). After excluding variants with low quality (quality score, <20) and low read counts (read counts, <5), 281,004 unique variants (SNV and indels) were collectively identified in the 10 individuals. After excluding homozygous variants (given the observed autosomal dominant inheritance pattern in PPPCD family 1), 108,844 heterozygous variants were

evaluated for allele frequency, revealing that 29,336 were novel or rare (MAF <0.5%). After filtering variants based on segregation with the affected phenotype, no novel or rare heterozygous coding region variants were present in all 6 affected individuals and not present in any of the 4 unaffected individuals. Although WES primarily targets the coding regions of the genome, the noncoding regions of the genome that are close to intron-exon junctions are also typically captured and sequenced. As such, screening of the 29,336 novel or rare heterozygous variants revealed 2 intronic variants, *PDZD8* c.872+10A>T (based on transcript NM_173791.4) and *GREB1L* c.4229-25T>C (based on transcript NM_001142966.2), that segregated with the affected phenotype in the 10 members of PPPCD family 1 who underwent WES (Table 3). Sanger sequencing that was performed to validate the WES results for these 2 intronic variants confirmed the results of WES in each of the 10 individuals. Sanger sequencing of *PDZD8* and *GREB1L* in the remaining 3 individuals of PPPCD family 1 who did not undergo WES (III:15, IV:6, IV:9) demonstrated that *PDZD8* c.872+10A>T continued to segregate with the affected status while *GREB1L* c.4229-25T>C did not.

To allow for a false positive and/or false negative call by WES for any particular variant in 1 individual, reanalysis of the WES data was performed using less stringent criteria for filtering variants (see Subjects and Methods), which led to the identification of 8 heterozygous novel or rare coding region variants present in 5 of 6 affected individuals and not present in any of the 4 unaffected individuals; and 3 heterozygous rare coding region variants present in 6 of 6 affected individuals and not present in more than 1 unaffected individual (Table 3). Sanger sequencing validation of these 11 total coding region variants did not identify any false positives; however, Sanger sequencing revealed that 3 variants, *OR2M5* c.773T>C, *PRDX3* c.568G>C and *LAMA3* c.1571G>A, were false negatives in 1 of the 6 affected individuals, thereby confirming each of these 3 variants to be present in all 6 affected individuals and not present in any of the 4 unaffected individuals. Sanger sequencing screening in the 3 additional family members who did not undergo WES revealed *OR2M5* c.773T>C and *PRDX3* c.568G>C continued to segregate with the affected status, whereas *LAMA3* c.1571G>A did not (Table 3). The *OR2M5* c.773T>C variant was predicted by SIFT to have an activating impact on protein function but was predicted to be benign or neutral by PolyPhen and Provean (Table 3). In contrast, *PRDX3* c.568G>C variant was predicted by SIFT, PolyPhen, and Provean to deleteriously impact protein function, and also obtained a CADD score of 31, which places this variant in the top 0.1% of deleterious substitutions in the human genome (Table 3).[12]

• **SCREENING OF *PDZD8, PRDX3,* AND *OR2M5* IN PPPCD FAMILIES 2 AND 3:** Given that *PDZD8* c.872+10A>T, *OR2M5* c.773T>C, and *PRDX3* c.568.G>C segregated with the affected status in PPPCD family 1, we performed Sanger sequencing of all 3 genes in 3 affected (I:1, II:1, II:4) and 2 unaffected (I:2, II:2) members of PPPCD family 2 and in 1 affected individual (II:1) and 1 unaffected individual (II:3) in PPPCD family 3 (Figure 1B and 1C). Sanger sequencing of the *OR2M5* coding region did not reveal a novel or rare variant in either family 2 or family 3. Sanger sequencing of *PDZD8* and *PRDX3* revealed the same *PDZD8* c.872+10A>T and *PRDX3* c.568G>C variants identified in PPPCD family 1 in the heterozygous state in the affected individuals and absent in the unaffected individuals of family 2 and family 3. The *PDZD8* and *PRDX3* variants are both located on chromosome 10 within ~2 Mb from each other. Based on a previously performed RNA-seq analyses of adult human corneal gene expression, both *PDZD8* and *PRDX3* are expressed in ex vivo keratocytes and endothelial cells, with Reads Per Kilobase of transcript, per Million mapped reads (RPKM) values of: 4.25 and 8.67 for *PDZD8*, respectively; and 8.43 and 33.91 for *PRDX3*, respectively.[18]

• **IMPACT OF *PDZD8* C.872 + 10A > T ON SPLICING:** In silico analysis performed using Human Splicing Finder version 3.1 predicted that the *PDZD8* c.872+10A>T variant activates an intronic cryptic donor splice site, potentially altering splicing. To determine whether the *PDZD8* c.872+10A>T variant does in fact alter splicing, an in vitro splice assay was performed by inserting a genomic sequence containing the *PDZD8* exon 1 and partial intron 1 (with either the c.872+10A>T variant or the wild-type sequence) in between 2 flanking fibronectin 1 (*FN1*) exons residing within a *FN1* minigene plasmid, which was subsequently transfected into HEK293T cells. Using cDNA generated from the transfected HEK293T cells, RT-PCR demonstrated the c.872+10A>T variant caused the loss of a transcript-splice product (denoted by a ~700-bp band) that was detected in the *FN1/PDZD8* minigene with the wild-type sequence (Supplemental Figure 1). Sequencing of the ~700-bp band revealed the c.325-c.872 region of *PDZD8* exon 1 spliced in between the 2 flanking *FN1* exons. Sequencing of the ~1,400-bp and ~400-bp bands revealed transcript products, flanked by the 2 minigene *FN1* exons, containing either the *PDZD8* 5′UTR and exon 1 regions; or a *FN1* exonic region (c.3797-4064, NM_212482), respectively (Supplemental Figure 1).

• **SCREENING OF *PRDX3, PDZD8,* AND *OR2M5* IN 2 PREVIOUSLY PUBLISHED PPPCD FAMILIES:** Genomic DNA samples were obtained from members of 2 previously reported PPPCD families: 3 affected individuals from PPPCD family 4 and 7 affected individuals from PPPCD family 5.[7] Screening of the *PDZD8* exon1/intron1 region in each of the affected individuals from both families did not reveal the c.872+10A>T variant. Screening of the *PDZD8* promoter and coding regions and the *OR2M5* coding region

TABLE 3. Variants Identified by WES

Affected Members Carrying the WES Variant	Unaffected Members Carrying the WES Variant	Chr	Position	Gene	Transcript ID	Transcript Variant	Amino Acid Change	dbSNP ID	GnomAD MAF (%)	SIFT/PolyPhen-2 Function Prediction	Confirmed by Sanger Sequencing to Be Present in 6 of 6 Affected Members and 0 of 4 Unaffecteds Members?	If Confirmed by Sanger Sequencing, Does the Variant Segregate into 3 Additional Family Members?
6 of 6	0 of 4	10	117374346	*PDZD8*	NM_173791.4	c.872+10A>T	-	rs201808439	0.006	-	Yes	Yes
6 of 6	0 of 4	18	21505785	*GREB1L*	NM_001142966.2	c.4229-25T>C	-	rs775835476	0.004	-	Yes	No
5 of 6	0 of 4	1	248145920	*OR2M5*	NM_001004690.1	c.773T>C	p.M258T	rs146014040	0.056	Activating/benign	Yes	Yes
5 of 6	0 of 4	5	194925	LRRC14B	NM_001080478.2	c.1117G>A	p.V373I	rs200063605	0.077	Tolerated/benign	No	-
5 of 6	0 of 4	5	10280458	CMBL	NM_138809.3	c.733A>C	p.M245L	rs182773279	0.086	Tolerated/benign	No	-
5 of 6	0 of 4	7	150692529	*GIMAP2*	NM_015660.2	c.243G>A	p.M81I	rs927523889	-	Activating/benign	No	-
5 of 6	0 of 4	8	8702651	CLDN23	NM_194284.2	c.253G>A	p.V85I	rs372410779	0.005	Tolerated/benign	No	-
5 of 6	0 of 4	10	17796225	TMEM236	NM_001098844.2	c.777C>A	p.N259K	rs1001234857	0.037	Tolerated/benign	No	-
5 of 6	0 of 4	10	119169326	*PRDX3*	NM_006793.4	c.568G>C	p.D190H	Note	-	Damaging/probably damaging	Yes	Yes
5 of 6	0 of 4	18	23784125	*LAMA3*	NM_001127717.2	c.1571G>A	p.R524H	rs201845068	0.036	Note/possibly damaging	Yes	No
6 of 6	1 of 4	1	226736078	*ITPKB*	NM_002221.3	c.1381C>T	p.P461S	rs35823273	0.396	Tolerated/benign	No	-
6 of 6	1 of 4	7	74120997	*LIMK1*	NM_002314.3	c.1729C>T	p.P577S	rs147218553	0.018	Tolerated/benign	No	-
6 of 6	1 of 4	7	76482982	*DTX2*	NM_001102596.1	c.743A>G	p.N248S	rs145151450	0.314	Tolerated/benign	No	-

Chr = chromosome; dbSNP = Single Nucleotide Polymorphism Database; gnomAD MAF = Genome Aggregation Database minor allele frequency; SIFT = Sorting Intolerant From Tolerant Database; WES = whole-exome sequencing.

in 2 affected individuals from both families failed to reveal a novel or rare variant. Screening of the *PRDX3* coding region in each of the affected individuals from both families identified the same c.568G>C variant in all 3 of the affected individuals of PPPCD family 4 but did not identify a novel or rare variant in PPPCD family 5.

• **IDENTIFICATION OF ANCESTRAL MINI-HAPLOTYPE IN FAMILIES 1-3:** Rare variants that are adjacent to the *PRDX3* c.568G>C variant were genotyped in the four PPPCD families that demonstrated the *PRDX3* c.568G>C variant to determine whether this variant likely arose from a common ancestor (Supplemental Figure 2). The same mini-haplotype was identified in the 3 previously unreported families (PPPCD families 1, 2, and 3) but not in PPPCD family 4, suggesting that the *PRDX3* c.568G>C variant likely arose from a common ancestor in PPPCD families 1-3 and independently in PPPCD family 4.

DISCUSSION

THE AIM OF THIS STUDY WAS TO PERFORM A THROUGH corneal phenotypic analysis and to elucidate the genetic basis of punctiform and polychromatic pre-Descemet corneal dystrophy after the identification of 3 unreported families. In order to corroborate the results of genetic analysis in these 3 families, we recruited members of 2 recently reported families for additional screening.[7] One of these families (Family 4) demonstrated the typical PPPCD phenotype, with localization of the opacities to the pre-Descemet posterior stroma, as was observed in the 3 unreported families. However, affected members of family 5 presented an atypical PPPCD phenotype in that the opacities were distributed throughout all levels of the corneal stroma, indicating that this family may have a dystrophy that is clinically and genetically distinct from *PRDX3*-associated PPPCD.[7] What is common to each of these 5 families and, indeed, to 8 of the 13 families reported to date is location in Spain or Spanish ancestry (Table 1). In addition, 4 of the 5 other families reported to date have been in Brazil (family origin not reported). Considering that Brazil and all South America have received strong immigration from the Iberian Peninsula since the XVI century, after the discovery of America, it is likely that the causative mutation(s) originated in the Iberian Peninsula centuries ago.

Our investigation identified 2 variants, *PRDX3* c.568G>C and *PDZD8* c.872+10A>T, that segregated with the affected status in multiple PPPCD pedigrees. *PRDX3* c.568G>C (p.Asp190His) is novel (not reported in the dbSNP database) and was identified in 4 of 5 pedigrees affected with PPPCD, with haplotype analysis indicating that this variant likely derived from an independent event in family 4. However, given the ~2-Mb distance between the 2 variants, the possibility that the *PRDX3* c.568G>C variant arose from the same founder in all 4 families cannot be ruled out. The *PDZD8* c.872+10A>T variant, identified in 3 of 5 PPPCD families, is not novel but is rare and was demonstrated to impact splicing in vitro; whether or not splicing was altered in vivo by this variant and was not simply an artifact of the in vitro splice assay, has yet to be determined. However, each of these 3 families in which it was identified also demonstrated the *PRDX3* c.568G>C variant, which is only ~2 Mb away from the *PDZD8* c.872+10A>T variant. Therefore, it is likely that these 2 variants on chromosome 10, along with the other rare variants within the shared mini-haplotype, were inherited from a common ancestor in PPPCD families 1-3. Given that both *PRDX3* c.568G>C and *PDZD8* c.872+10A>T were identified in PPCD families 1-3 that likely share a common ancestor, but the novel *PRDX3* c.568G>C variant was also found in a fourth unrelated PPPCD pedigree, *PRDX3* is likely the causative gene for PPPCD.

The *PRDX3* gene belongs to the thioredoxin family of peroxidases and encodes a mitochondrial antioxidant peroxidase that is responsible for regulating mitochondrial reactive oxygen species.[19–21] Overexpression of *PRDX3* has been reported in various cancers, whereas knockdown of *PRDX3* was demonstrated to increase mitochondrial DNA oxidation, and silencing of *PRDX3* promoted enhanced invasive properties in HepG2 cells.[22–26] Interestingly, a significant decrease of PRDX3 protein expression was reported in corneal endothelium derived from patients affected with Fuchs endothelial corneal dystrophy (FECD) compared to healthy controls, suggesting that corneal endothelial cells affected with FECD are less able to withstand oxidant-induced damage, possibly contributing to the pathogenesis of the disease.[27] In the same report, although the PRDX3 protein was shown to be expressed in normal corneal endothelium, the PRDX3 protein was not expressed in either normal corneal stroma or epithelium.[27] Although the present identification of *PRDX3* expression in ex vivo human corneal endothelial cells using RNA-seq corroborates that report, *PRDX3* was found in this study to be expressed in corneal stromal keratocytes, again using RNA-seq data.[18] Functional studies will elucidate how the c.568G>C variant impacts the expression, localization, and function of PRDX3 in the cornea and whether or not the polychromatic crystalline-like opacities located in the stromal extracellular matrix are byproducts of aberrant PRDX3 proteins. To date, histopathologic examination of only 1 corneal button obtained post-mortem from an affected individual has been performed, which indicated that the opacities may represent focal lipid accumulations.[28]

According to the second edition of the IC3D classification of corneal dystrophies, PPPCD is currently classified as a subtype of PDCD as a category 4 dystrophy, indicating that "the evidence for it, being a distinct entity is not yet convincing."[8] Although the presence of punctate opacities anterior to Descemet membrane is a common feature of

each subtype of PDCD, the PDCD subtypes differ in terms of inheritance, age of onset and morphology of the deposits. This study presents a comprehensive clinical characterization of PPPCD and reports the association between a segregating *PRDX3* missense variant in 4 PPPCD pedigrees and an autosomal dominant inheritance pattern. Therefore, it is suggested that PPPCD may be considered a distinct, inherited disorder and reclassified as a category 1 dystrophy, defined as a "well-defined corneal dystrophy in which the gene has been mapped and identified and the specific mutations are known."[8]

ALL AUTHORS HAVE COMPLETED AND SUBMITTED THE ICMJE FORM FOR DISCLOSURE OF POTENTIAL CONFLICTS OF INTEREST and none were reported.

Funding/Support: This work was carried out in the framework of the Red Temática de Investigación Cooperativa en Salud (RETICS), reference number RD16/0008/0012, financed by the Instituto Carlos III, Madrid, Spain, General Subdirection of Networks and Cooperative Investigation Centers (R&D&I National Plan 2008-2011) and the European Regional Development Fund (Fondo Europeo de Desarrollo Regional [FEDER]). Support was also provided by National Eye Institute grants R01 EY022082 (to A.J.A.), P30 EY000331 (core grant), the Walton Li Chair in Cornea and Uveitis (to A.J.A.), the Stotter Revocable Trust and an unrestricted grant to Stein Eye Institute from Research to Prevent Blindness.

Financial Disclosures: The authors have reported that they have no relationships relevant to the contents of this paper to disclose.

The authors thank Dr. Carmen Cardona (Vissum Corporación, Alicante, Spain) for supporting the clinical assessment of the families included in this study.

REFERENCES

1. Fernandez-Sasso D, Acosta JE, Malbran E. Punctiform and polychromatic pre-Descemet's dominant corneal dystrophy. *Br J Ophthalmol* 1979;63:336–338.
2. Lagrou L, Midgley J, Romanchuk KG. Punctiform and polychromatophilic dominant pre-descemet corneal dystrophy. *Cornea* 2016;35:572–575.
3. Dolz-Marco R, Gallego-Pinazo R, Pinazo-Duran MD, Diaz-Llopis M. Crystalline subtype of pre-descemetic corneal dystrophy. *J Ophthalmic Vis Res* 2014;9:269–271.
4. Coelho LM, Muinhos GK, Tanure MAG, Almeida HGd, Sieiro RdO. Distrofia policromática posterior da córnea. *Revista Brasileira de Oftalmologia* 2015;74:186–188.
5. Tzelikis PFdM, Santos URd, Tanure MAG, Trindade FC. Distrofia corneana policromática posterior. *Revista Brasileira de Oftalmologia* 2007;66:262–266.
6. Lisch W, Weidle EG. [Posterior crystalline corneal dystrophy]. *Klin Monbl Augenheilkd* 1984;185:128–131.
7. Henríquez-Recine MA, Marquina-Lima KS, Vallespín-García E, et al. Heredity and in vivo confocal microscopy of punctiform and polychromatic pre-Descemet dystrophy. *Graefes Arch Clin Exp Ophthalmol* 2018;256:1661–1667.
8. Weiss JS, Moller HU, Aldave AJ, et al. IC3D classification of corneal dystrophies—edition 2. *Cornea* 2015;34:117–159.
9. Ng PC, Henikoff S. SIFT: predicting amino acid changes that affect protein function. *Nucleic Acids Res* 2003;31:3812–3814.
10. Adzhubei I, Jordan DM, Sunyaev SR. Predicting functional effect of human missense mutations using PolyPhen-2. *Curr Protoc Hum Genet* 2013;7:Unit7.20.
11. Kircher M, Witten DM, Jain P, O'Roak BJ, Cooper GM, Shendure J. A general framework for estimating the relative pathogenicity of human genetic variants. *Nat Genet* 2014;46:310–315.
12. Rentzsch P, Witten D, Cooper GM, Shendure J, Kircher M. CADD: predicting the deleteriousness of variants throughout the human genome. *Nucleic Acids Res* 2019;47(suppl D1):D886–D894.
13. Choi Y, Sims GE, Murphy S, Miller JR, Chan AP. Predicting the functional effect of amino acid substitutions and indels. *PLoS One* 2012;7:e46688.
14. Desmet FO, Hamroun D, Lalande M, Collod-Beroud G, Claustres M, Beroud C. Human splicing finder: an online bioinformatics tool to predict splicing signals. *Nucleic Acids Res* 2009;37:e67.
15. Baralle M, Baralle D, De Conti L, et al. Identification of a mutation that perturbs NF1 agene splicing using genomic DNA samples and a minigene assay. *J Med Genet* 2003;40:220–222.
16. Pagani F, Stuani C, Tzetis M, et al. New type of disease causing mutations: the example of the composite exonic regulatory elements of splicing in CFTR exon 12. *Hum Mol Genet* 2003;12:1111–1120.
17. Muro AF, Caputi M, Pariyarath R, Pagani F, Buratti E, Baralle FE. Regulation of fibronectin EDA exon alternative splicing: possible role of RNA secondary structure for enhancer display. *Mol Cell Biol* 1999;19:2657–2671.
18. Frausto RF, Le DJ, Aldave AJ. Transcriptomic analysis of cultured corneal endothelial cells as a validation for their use in cell-replacement therapy. *Cell Transplant* 2016;25:1159–1176.
19. Li L, Shoji W, Takano H, et al. Increased susceptibility of MER5 (peroxiredoxin III) knockout mice to LPS-induced oxidative stress. *Biochem Biophys Res Commun* 2007;355:715–721.
20. Shibata E, Nanri H, Ejima K, et al. Enhancement of mitochondrial oxidative stress and up-regulation of antioxidant protein peroxiredoxin III/SP-22 in the mitochondria of human pre-eclamptic placentae. *Placenta* 2003;24:698–705.
21. Lee S, Wi SM, Min Y, Lee KY. Peroxiredoxin-3 is involved in bactericidal activity through the regulation of mitochondrial reactive oxygen species. *Immune Netw* 2016;16:373–380.
22. Liu Z, Hu Y, Liang H, Sun Z, Feng S, Deng H. Silencing PRDX3 inhibits growth and promotes invasion and extracellular matrix degradation in hepatocellular carcinoma cells. *J Proteome Res* 2016;15:1506–1514.
23. Hu JX, Gao Q, Li L. Peroxiredoxin 3 is a novel marker for cell proliferation in cervical cancer. *Biomed Rep* 2013;1:228–230.
24. Kinnula VL, Lehtonen S, Sormunen R, et al. Overexpression of peroxiredoxins I, II, III, V, and VI in malignant mesothelioma. *J Pathol* 2002;196:316–323.

25. Noh DY, Ahn SJ, Lee RA, Kim SW, Park IA, Chae HZ. Overexpression of peroxiredoxin in human breast cancer. *Anticancer Res* 2001;21:2085–2090.
26. Whitaker HC, Patel D, Howat WJ, et al. Peroxiredoxin-3 is overexpressed in prostate cancer and promotes cancer cell survival by protecting cells from oxidative stress. *Br J Cancer* 2013;109:983–993.
27. Jurkunas UV, Rawe I, Bitar MS, et al. Decreased expression of peroxiredoxins in Fuchs' endothelial dystrophy. *Invest Ophthalmol Vis Sci* 2008;49:2956–2963.
28. Croxatto JF-SD, Malbran ES. Clinicopathologic findings in punctiform and polychromatic pre-Descemet's corneal dystrophy. *Invest Ophthalmol Vis Sci* 2002;43. e-abstract 1724.